

A numerical trim methodology study for the Kriso Container Ship with bulbous bow form variation

M. Maasch

E. Shivachev

A. H. Day

O. Turan

Department of Naval Architecture, Ocean and Marine Engineering, University of Strathclyde, Glasgow, UK

ABSTRACT: The application of Computational Fluid Dynamics (CFD) is the fastest developing area in marine fluid dynamics as an alternative to Experimental Fluid Dynamics (EFD). While EFD employs well-established methods for predicting a ship's performance, CFD is still challenged to reach a reliable level of accuracy in a reasonable amount of time. In the present study, this issue is addressed in the context of trim optimization by exploring the combination of time-inexpensive potential flow simulations with high-fidelity Unsteady Reynolds-averaged Navier-Stokes (URANS) simulations. This approach allowed covering a broad fore body design space by running a large number of potential flow simulations while at the same time important flow effects due to viscous forces were included by running URANS simulations over the full speed range for a small set of simulations. The KCS baseline design results were validated against an experimental towing tank dataset ensuring a valid CFD setup and thus demonstrating its competitiveness to EFD.

1 INTRODUCTION

Fluctuating fuel prices and the newly adopted mandatory measures by the International Maritime Organization (IMO) to reduce emissions have been driving the shipping industry to become more efficient. Energy efficiency is becoming an integral part of ship design. Ship hull forms are traditionally designed to perform best for one operating condition (design speed and design draft); however, cargo ships often operate in off-design conditions.

One of the methods to improve the hydrodynamic performance of ships when sailing at a speed different to the design speed or in adverse loading conditions is to operate the ship at a trim angle. This allows bringing certain ship hull geometry features, such as the bulbous bow, the stern bulb or the transom back into the design position (in reference to the design conditions). The potential of further improving the energy efficiency of ships when operating in trimmed conditions could be investigated by optimising those hull parts.

Changing the bulbous bow shape in order to adapt its design to the adverse operating conditions is a challenging task, as one needs to make sure that the new geometry also works in the design conditions. The new design should result in a compromise that works better on average over a realistic set of loading conditions than the original hull. Ideally, the hull geometry change should also be restricted to a small part of the ship so that the new design can be applied as a

retrofit option. Ship hull optimization is a complex and important aspect of ship design. The available scope of ship design optimization largely extended with the use of numerical tools, both for Computer Aided Design (CAD) and Computational Fluid Dynamics (CFD). Various marine software packages include some functionality to alter the shape of the numerical hull surface representation such as points-based modification of standard surface models (e.g. NURBS surfaces) or parametric geometry objects. The overall goal of ship geometry optimization is to improve the operational performance, often targeting on a low fuel consumption. An indication of an improved performance can be given by the ship hull resistance reduction. Ship resistance was traditionally predicted by towing tank experiments only. However, with the rapid developments in computer technology, numerical ship hull design became widely used and nowadays assists or even replaces experimental towing tests. Still, numerical results are compared to the experimental data if available for validation purposes.

Both topics, numerical trim optimization and numerical bulbous bow optimization, independently, have already been investigated within various studies using the KCS and other ship geometries. Filip et al (2014) presented a bulbous bow retrofit analysis for the KCS container ship under slow steaming conditions using Reynolds-averaged Navier-Stokes Equations (RANSE) simulations for a small number of design variants, certainly limited by the extensive

simulation time. Wagner et al (2014) carried out a scenario-based optimization of the KCS bulbous bow for four different operating conditions at various speeds and drafts using a potential flow solver. This allowed creating a high number of design variants; however, Wagner et al further suggested to include sophisticated RANSE simulations for better results accuracy and to validate the potential solver results. Vroegrijk et al (2015) performed a full-scale bulbous bow optimization on a container ship by using a combination of potential flow and RANSE simulations. For the ship at different drafts and speeds, the results showed that the potential flow simulations were not able to accurately predict the performance trend between different bulbous bow variants. Hence, Vroegrijk et al concluded that only RANSE simulations should be used within in a bulbous bow optimization study. FORCE Technology (Reichel et al, 2014) performed an extensive series of experimental trim model tests for different ship types. This study concluded that the change in trim mostly affected the wave making resistance component of the total resistance. As mentioned before, by trimming the ship, the bulbous bow and other energy saving geometry features are rotated back into an ideal operational point. This conclusion allows suggesting that a potential flow solver could be well suited for a trim study, as it can quickly estimate the wave making resistance.

Following the above review of previous studies, this paper presents a trim optimization study in combination with a bulbous bow retrofit for both design and adverse operating conditions using the benchmark Kriso Container Ship (KCS).

The performance of the KCS was calculated using potential flow simulations as well as URANS simulations. Furthermore, simulation results were validated by experimental tests.

2 TRIM STUDY METHODOLOGY

Based on the Kriso Container Ship (KCS) benchmark hull, the setup of this trim study consisted of three stages. At stage 1, the bulbous bow of the KCS hull geometry was partially parametrised within the parametric CAD modeller of the software CAESSES by FRIENDSHIP Systems. At stage 2, the original KCS and 39 KCS bulbous designs were simulated in a virtual towing tank using the marine flow code Shipflow (SHF) by Flowtech AB for steady ship hydrodynamics. At stage 3, based on the wave making resistance at seven trim angles and three operational speeds, predicted by the potential flow code, one of the best design candidates was chosen to be simulated using the RANSE code STAR-CCM+ by SIEMENS. Furthermore, the original KCS was also simulated using the RANSE code to perform a comparison to the experimental results. Figure 1 shows the structure for the proposed methodology of this trim study.

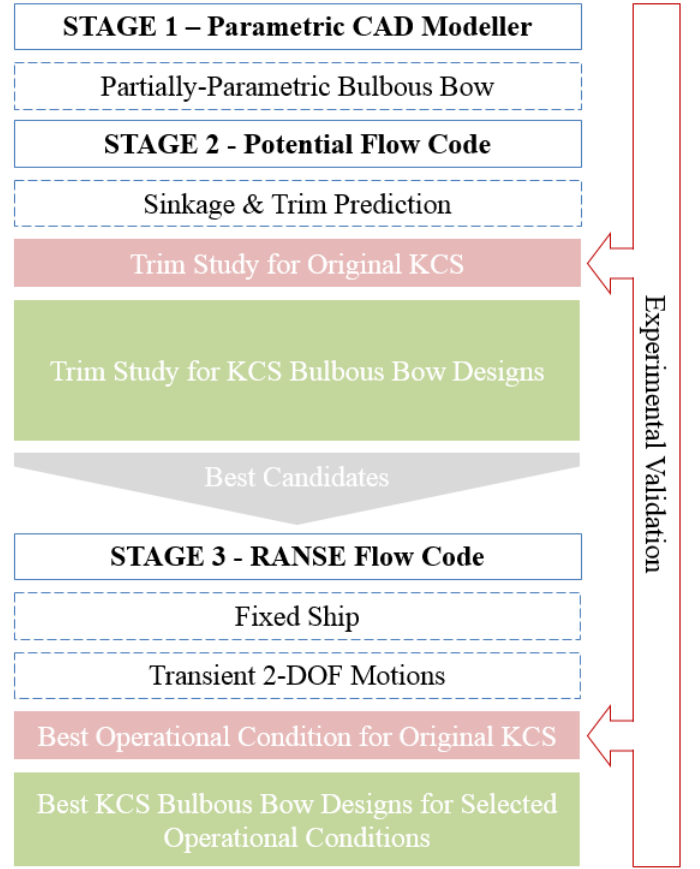


Figure 1. Trim study methodology

The shown strategy fulfilled two purposes. First, the most beneficial trim angle for three operational speeds could be derived for the original KCS and validated by experimental tests. Second, it could be estimated how much the KCS performance would benefit from a bulbous bow retrofit for different speeds. Therefore, the total resistance difference $\Delta R_{TM}^{v,\theta}$ of each design to the original KCS was calculated at a given speed and trim angle (Eq. 1).

$$\Delta R_{TM}^{v,\theta} = R_{TM,Original}^{v,\theta} - R_{TM,Modified}^{v,\theta} \quad (1)$$

The operational profile was defined by weighting factors t_{vi} (Eq. 2), representing the time spent in each speed.

$$\sum_0^i t_{vi} = 1 \quad (2)$$

Finally, the total resistance improvement $\Delta R_{TM}^{Profile}$ for a specific operational profile (Eq. 3) could be derived.

$$\Delta R_{TM}^{Profile} = \Delta R_{TM}^{v1} t_{v1} + \Delta R_{TM}^{v2} t_{v2} + \Delta R_{TM}^{v3} t_{v3} \quad (3)$$

2.1 Parametric Computer Aided Design of the KCS

The partially parametric KCS geometry model is based on the publicly available IGES file (http://www.simman2008.dk/KCS/kcs_geometry.htm) with the specifications given in Table 1. In order to allow a feasible variation of the KCS bulbous bow shape, a partially parametric modelling approach based on the deformation of image objects of the KCS hull was chosen. Although not as flexible as the fully parametric modelling approach, the partially parametric modelling approach is well suited for the modification of local geometry features of an already existing geometry. To make this study an example of a potential bulbous bow retrofit the area of shape modification was restricted to the bulb and a small part of the underwater fore ship. Figure 2 illustrates the KCS in starboard view. The area of modification is highlighted in golden colour.

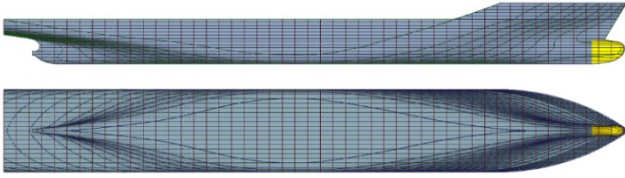


Figure 2. KCS hull geometry (starboard and bottom-up view)

Table 1 lists the KCS model properties for full scale and model scale. The model scale geometry of the original KCS hull was built for experimental testing in the Kelvin Hydrodynamics Laboratory at the University of Strathclyde.

Table 1. KCS hull properties

Dimensions	Full Scale	Model Scale
Scale	1	75
LPP (m)	230	3.0667
BWL (m)	32.2	0.4293
D (m)	19	0.2533
T (m)	10.8	0.144
Displacement (m ³)	52030	0.1203
S w/o rudder (m ²)	9530	1.651
CB	0.651	0.651
CM	0.985	0.985

Three geometry shift functions were applied to the bulbous bow, which allowed changing its length (dx), width (dy) and tip height (dz). Figure 3 shows an example of each shift function independently by comparing the original KCS fore ship (grey colour) with the modified shape (golden colour). Care was taken that the geometry modification had no effect on the fair transition of the bulbous bow into the fore ship shape. The geometry setup was then coupled with the variation algorithm SOBOL (available in CAESSES)

that quasi-randomly created 40 variants within the chosen boundaries.

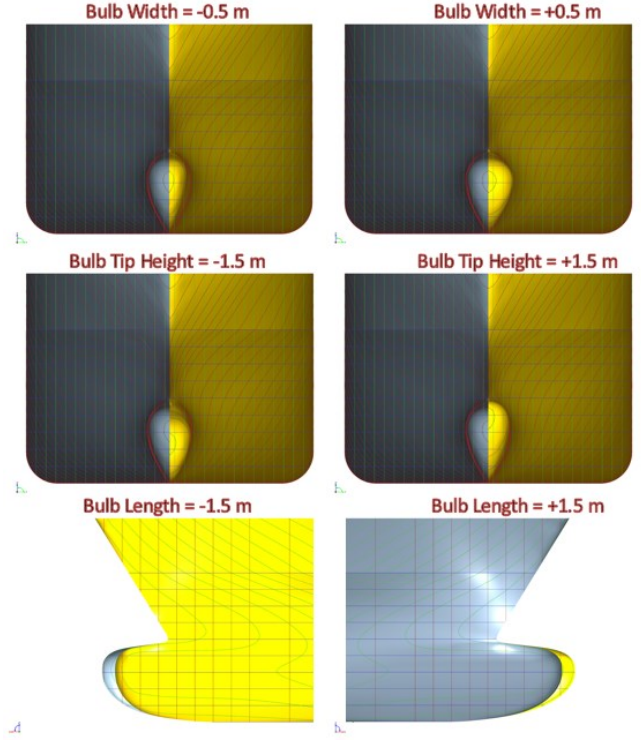


Figure 3. Geometry shifts of the KCS bulbous bow

2.2 Scope of operational conditions

The present trim study comprises of 40 bulbous bow design variants (including the original KCS design), simulated in seven different trim angles for three different speeds. The trim of a floating ship is defined as the difference in forward draft T_f and aft draft T_a , and can be expressed as distance t in unit meter (Eq. 4) or as angle θ in unit degree (Eq. 5).

$$t = T_f - T_a \quad (4)$$

$$\tan(\theta) = \frac{T_f - T_a}{L_{pp}} \quad (5)$$

The displacement of the KCS was kept constant throughout the whole study. For specifying the range of trim angles, only those cases were considered that would allow an operation in self-propulsion conditions with the propulsor sufficiently submerged. At a constant displacement, higher bow-down trim angles would cause the propulsor to get closer to the free surface, resulting in a loss in operating performance. Hence, the propeller tip clearance, i.e. the distance from the top propeller blade tip in top position to the undisturbed water level in relation to the propeller diameter, was monitored. As a threshold, a propeller tip clearance of 15% of propeller diameter was set which yielded a critical bow down trim angle of $\theta = 0.75^\circ$ (see Figure 4).

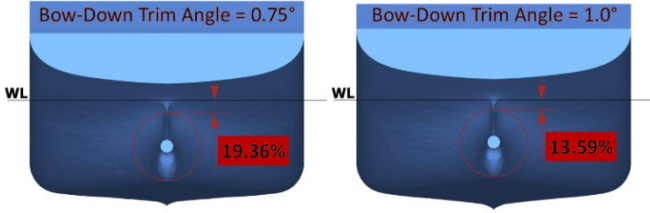


Figure 4. KCS propeller tip clearance (as percentage of propeller diameter)

The bow-up trim angle range is often not limited by the propeller tip clearance as the propulsor moves away from the free surface. Hence, the trim angle range was kept variable. During the computation of KCS in bow-up conditions the analysis yielded an increase in total resistance which led to the decision to restrict the bow-up trim angle range to -0.75° as no further improvement was expected. Thus, the final trim angle range was set to $\pm 0.75^\circ$.

The three chosen operational speeds represented the KCS slow-steaming speed of 18 knots (v_1), a medium speed of 21 knots (v_2) and the KCS design speed of 24 knots (v_3), here given as full-scale speeds. Defined by the above stated limits the set of performed simulations consisted of 21 operational conditions for 40 KCS designs. The created results pool served as basis to derive a performance trend of the KCS for different operating profiles. The below points summarise the scope of the present trim study:

- 40 different hull variants were created (including the original KCS)
- Those variants were used to perform potential flow code simulations
- At three speeds at $Fn = 0.195, 0.227, 0.269$
- At seven trim angles from $\theta = -0.75^\circ$ to 0.75° in steps of $\theta = 0.25^\circ$
- The geometry of the original KCS and the best bulbous bow design candidate was used to perform URANS simulations
- Numerical results for the original KCS geometry were validated against experimental data

2.3 Experimental data

Prior to the presented numerical trim study, experimental tests were performed for the KCS model for various operational conditions. The tests were carried out in the Kelvin Hydrodynamics Laboratory of the University of Strathclyde. The experimental setup and the results were presented by Shivachev (2017). For this study, the results were further post-processed by calculating the non-dimensional resistance coefficients for a corrected water temperature of 15°C following procedures proposed by the ITTC (ITTC 7.5-02-02-01). For the measured fresh water temperature that defined the water density ρ_M and kinematic viscosity ν_M , the monitored total resistance force of the

KCS model R_{TM} at a carriage speed v_M was converted to its non-dimensional total resistance coefficient c_{TM} considering the hydrostatic wetted surface S_M (Eq. 6).

$$c_{TM} = \frac{R_{TM}}{0.5 \rho_M S_M v_M^2} \quad (6)$$

The frictional resistance coefficient $c_{FM,ITTC}$ was calculated by the ITTC-1957 frictional correlation line (Eq. 8) for the model Reynolds number Re_M (Eq. 7), considering the hydrostatic water line length $L_{M,WL}$.

$$Re_M = \frac{v_M L_{M,WL}}{\nu_M} \quad (7)$$

$$c_{FM,ITTC} = \frac{0.075}{(\log Re_M - 2)^2} \quad (8)$$

The wetted surface (see Eq. 6) and the waterline length of the KCS (see Eq. 7) varied for each calculated trim angle as shown in Figure 5.

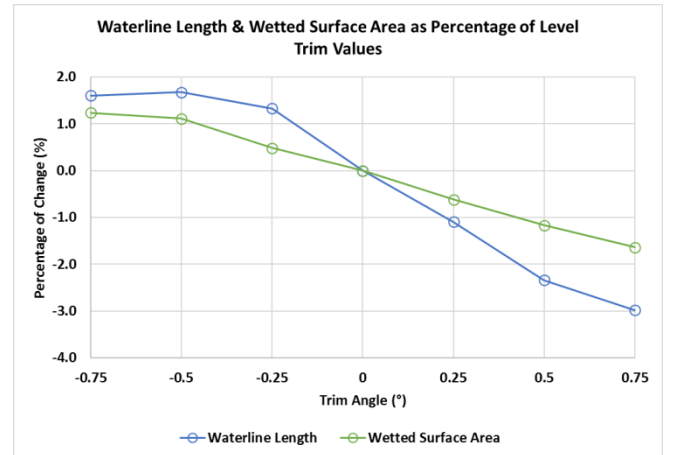


Figure 5. Variation of waterline length and wetted surface due to trim

The residuary resistance coefficient c_{RM} , which was assumed to equate to the wave making resistance coefficient $c_{RM} = c_W$ (Eq. 9), was defined as difference of the total resistance coefficient and the frictional resistance coefficient. The form factor k was determined by the performed Prohaska model tests at level trim to $(1 + k) = 1.0118$.

$$c_W = c_{TM} - c_{FM,ITTC}(1 + k) \quad (9)$$

In order to correct the viscous effects of the measured results to a water temperature of 15°C , the frictional resistance coefficient $c_{FM,ITTC}^{15^\circ\text{C}}$ (Eq. 11) was re-

calculated by considering the model Reynolds Number $Re_M^{15^\circ C}$ (Eq.10) for the kinematic viscosity $\nu_M^{15^\circ C}$ at $15^\circ C$.

$$Re_M^{15^\circ C} = \frac{v_M L_{M,WL}}{\nu_M^{15^\circ C}} \quad (10)$$

$$c_{FM,ITTC}^{15^\circ C} = \frac{0.075}{(\log Re_M^{15^\circ C} - 2)^2} \quad (11)$$

This yielded the corrected total resistance coefficient $c_{TM}^{15^\circ C}$ (Eq. 12) and finally the corrected total resistance $R_{TM}^{15^\circ C}$ at $15^\circ C$ (Eq. 13).

$$c_{TM}^{15^\circ C} = c_{FM,ITTC}^{15^\circ C}(1 + k) + c_W \quad (12)$$

$$R_{TM}^{15^\circ C} = 0.5 c_{TM}^{15^\circ C} \rho_M S_M v_M^2 \quad (13)$$

The temperature corrected total resistance of the experiments for the measured trim angles at the three speeds is given in Table 2.

Table 2. Experimental total resistance at $15^\circ C$

Trim ($^\circ$)	Total Resistance (N) at $15^\circ C$		
	Fn=0.195	Fn=0.227	Fn=0.269
-0.6	4.444	5.856	7.759
-0.25	4.232	5.651	7.659
0	4.166	5.607	7.512
0.25	4.114	5.478	7.427
0.6	4.142	5.568	7.632

The total resistance was used to validate both the potential flow and the URANS simulations.

2.4 Numerical simulation setups

The potential code simulations (stage 2) were performed using a Rankine panel code to calculate the wave making resistance coefficient c_W from transverse wave cuts on the disturbed free surface (Flowtech International AB, 2017). A panel mesh study was performed for the original KCS hull geometry in level trim conditions for three speeds. Table 3 shows the resolution of each part mesh for a coarse mesh, a medium mesh and a fine mesh setup.

Table 3. Panel mesh resolution for mesh study

Mesh	Total	KCS hull				Free Surface
		Aft	Boss	Main	Bulb	
Coarse	3603	70	25	792	70	2646
Medium	8996	192	40	1995	204	6605
Fine	13904	300	50	3024	315	10215

Figure 6 illustrates the panel mesh setup for the KCS hull parts and the free surface.

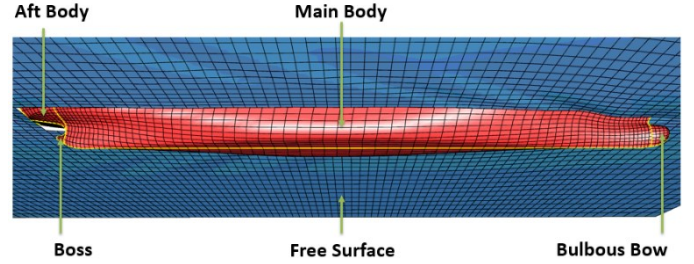


Figure 6. Panel mesh visualisation (coarse)

The results for the wave making resistance coefficient c_W , computed on three meshes of different density, were used to calculate the total resistance (Eq. 12) which was then compared to the experimental measurements. Although the total resistance predicted by the panel mesh code converged towards the experimental results, the error of around 5% was considered too high. The SHF wave cut method gave an accurate trend prediction for the wave making resistance coefficient compared to the experiments, but it failed to calculate the coefficient within the correct range of magnitude. The observed magnitude offset is a known effect of the wave cut method (Flowtech User Support, 2017). Given that the same mesh setup, i.e. free surface panel mesh resolution for the wave cut calculations, was used throughout all simulations, the c_W -magnitude offset was considered to be similar for each calculated simulation result.

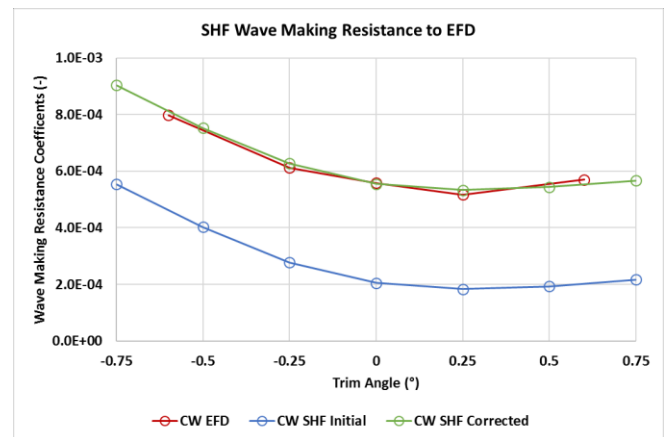


Figure 7. Wave making resistance coefficient correction

Since a rather accurate prediction of the impact of a bulbous variation on the total ship resistance was an

important target of this study, the coefficient was corrected in magnitude by a value of $c_{W,Correction} = 3.5 \cdot 10^{-4}$ for each calculated variant. The result of the correction for the original KCS geometry at slow steaming speed is shown in Figure 7. The applied correction allowed recalculating the results for the mesh study, which led to a difference of under 1% compared to the experiments for the fine panel mesh.

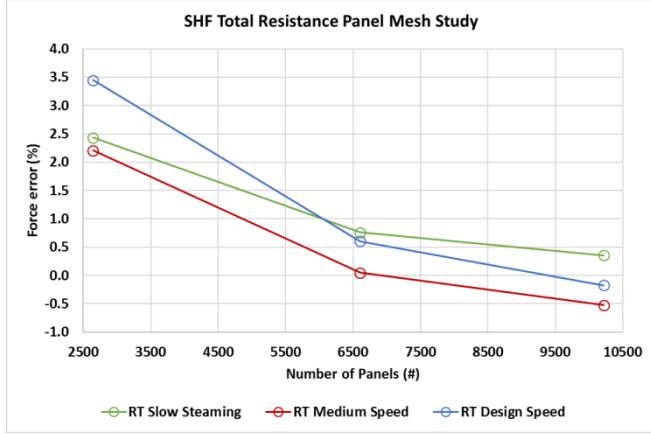


Figure 8. Percentage error of total resistance for three speeds predicted on three panel mesh resolutions

The convergence trend of the mesh study for three speeds is shown in Figure 8. The fine panel mesh setup was chosen for the trim study. In total, 840 potential flow simulations were carried out, covering the original KCS geometry and 39 bulbous bow designs.

The RANSE code simulations (stage 3) were used to compute the total resistance of the KCS directly. The numerical mesh and the solver setup summarised below were already discussed in Shivachev (2017) and remained unchanged.

- Model scale at 1/75 to original size of the KCS
- Hexahedral mesh of around 0.6 million cells in a cuboid domain
- Half domain setup with the centre plane (symmetry plane) along the ship keel line
- Local mesh refinements around the KCS hull and on the free surface to provide a higher resolution of local flow phenomena
- All- y^+ treatment with a target of $y^+ > 30$
- RANSE solver with a $k-\epsilon$ turbulence model
- Implicit unsteady 1st-order time model with a time step of $\Delta t = 0.01 L_{M,WL}/v_M$, following the recommendations of the ITTC (2011)
- Volume of Fluid model to capture the free surface interface between two immiscible fluids, i.e. water and air
- 2-DOF dynamic ship motions were resolved using the Dynamic Fluid Body Interaction (DFBI) module

The original KCS geometry was simulated at design speed over the chosen trim angle range with and

without an active DFBI model, i.e. with a fixed hull and the hull free for sinkage and trim. Therefore, the simulations were started with a fixed ship. After the convergence of the total resistance, the DFBI motion model was activated. Again, the simulation results, i.e. the total resistance and the dynamic sinkage and trim motions, were allowed to converge. The same approach was followed for the best KCS bulbous bow design, which was simulated for all three speeds over the chosen trim angle range in order to allow for a performance trend analysis. In total, 28 CFD simulations were carried out.

3 NUMERICAL RESULTS

As outlined in Section 2, the numerical results pool, consisting of 868 simulations, was first assessed regarding the performance of the original KCS geometry (Section 3.1). Therefore, the numerical results were compared against the experimental measurements for each speed and trim angle, thus proving a valid numerical setup. The results of the potential flow simulations (SHF), i.e. wave profiles, the wave making resistance and the total resistance, were analysed in order to explain the differences in performance over the trim angle range. Finally, the RANSE simulation results were compared to the potential flow code results and to the experimental measurements.

Section 3.2 presents the results pool assessment for the KCS bulbous bow designs in comparison to the original KCS geometry for each trim angle. By assessing the impact of the bulbous design change on the wave making resistance, the minimization of energy losses associated with the generation of waves could be estimated. Then, the same approach was chosen to evaluate the total resistance reduction. Finally, the best KCS bulbous design was simulated using the RANSE code to check the validity of the potential flow simulations and to include the impact of viscous forces.

3.1 Original KCS geometry

The results assessment for the original KCS geometry was performed to derive the most beneficial trim angle and to validate the numerical results with the experimental data. Therefore, the first part of the results pool evaluation focused on the total resistance variation. Figure 9 shows a direct comparison of the numerical and the experimental results over the trim angle range for three speeds. It can be noted that the trend and the magnitude of the numerical results agrees well with the experiments. For both data sets a bow-down trim of $\theta = 0.25^\circ$ seems to be the most beneficial condition.

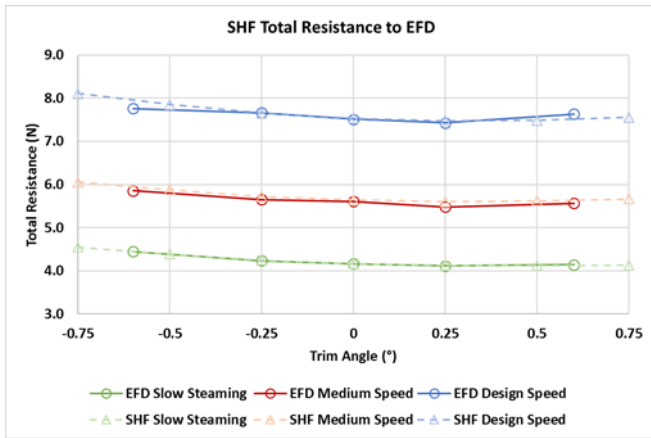


Figure 9. Total resistance (SHF) validation

The slight difference in the results originated from the corrected wave making resistance prediction of the panel code as the frictional resistance component, based on the ITTC-1957 frictional correlation line (Eq. 8), was equal for both the numerical and the experimental results.

Figure 10 shows the free surface elevation at design speed over the trim range along the KCS hull trough the domain. The KCS forepeak is positioned at $x/Lpp = 0$, the aft peak at $x/Lpp = 1$. For the bow-down trim conditions, the KCS generates a slightly higher bow wave. The stern wave profiles at the aft peak are higher for the bow-down trim as well; however, the disturbances faded more quickly downstream compared to the bow-up trim condition profiles. Hence, the prediction of shallower waves for bow-down conditions resulted in a reduced wave-making resistance calculated by the wave cut method.

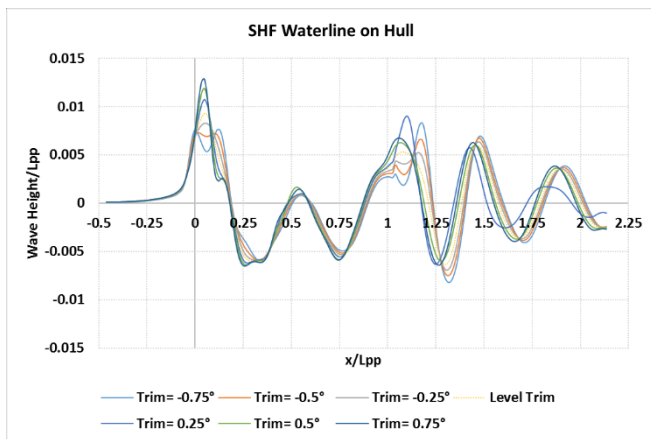


Figure 10. Waterline elevation on the KCS hull

The same trend can be observed in Figure 11, which shows the free surface elevation at $y/Lpp = 0.1$ through the computational domain. For steady-state flow simulations, those wave cuts can be interpreted as flow pattern traveled downstream from the hull.

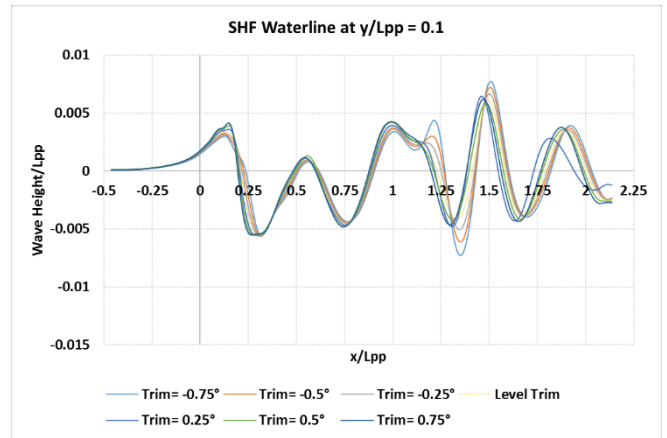


Figure 11. Waterline elevation on KCS hull

Whereas the bow wave has settled for all trim conditions while traveling downstream, the wave profile in the wake of the ship at the position $x/Lpp \approx 1.5$ remains pronounced which results from the hull stern wave (observed in Figure 10 at $x/Lpp \approx 1.4$). This effect is also shown in Figure 12, which illustrates a comparison of the free surface for $\theta = -0.75^\circ$ (RHS) and $\theta = 0.25^\circ$ (LHS).

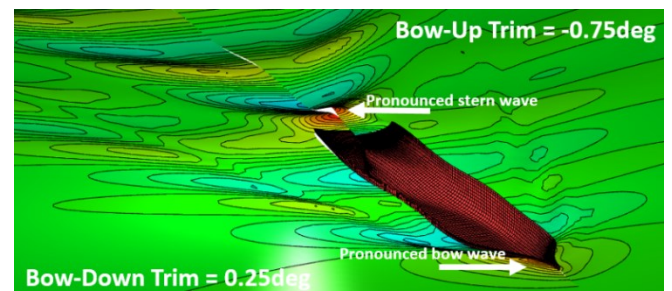


Figure 12. Free surface contour plots comparison

The above figure also shows a pronounced bow wave for the bow-down trim, which suggests that an adapted bulbous bow could in fact further improve this operational condition.

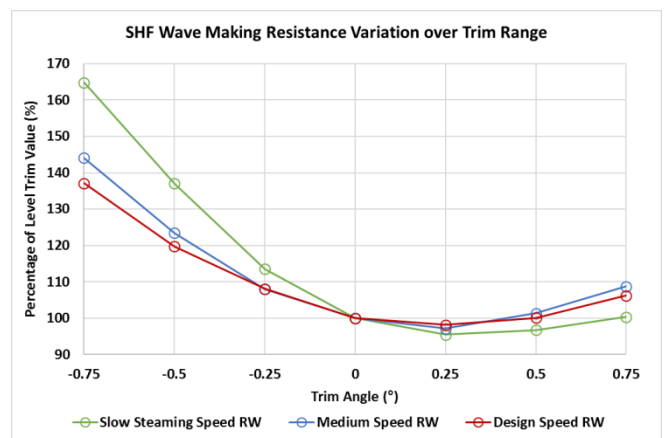


Figure 13. Wave making resistance comparison to level trim value over trim range

Figure 13 compares the wave making resistance at each trim angle against the level trim predictions. For bow-up trim conditions, the wave making resistance

shows a large increase of up to 65% above level trim. For $\theta = 0.25^\circ$ bow-down trim, the wave making resistance finds its lowest value, which again agrees well with the experimental findings.

Figure 14 shows the impact of the trim variation on the total resistance. Due to the influence of the waterline length and the wetted surface on the frictional resistance component (see Figure 5), the total resistance shows minor trend differences for bow-up trim compared to the wave making resistance.

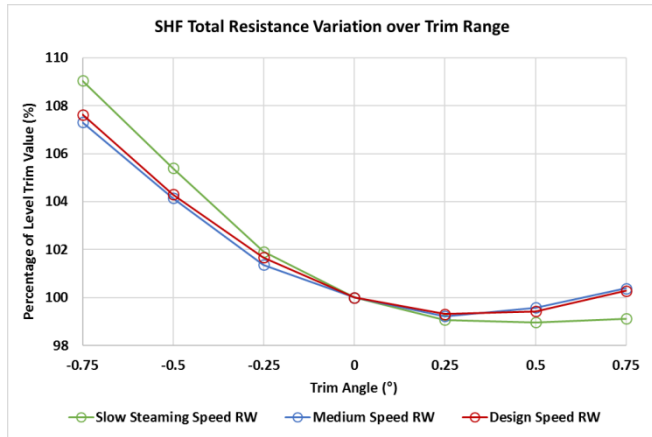


Figure 14. Total resistance comparison to level trim value over trim range

Due to the low fraction of the wave making resistance on the total resistance, for the original KCS between 5% for the slow steaming speed up to 11% for the design speed, larger improvements in the wave making resistance only resulted in small improvements in the total resistance. In agreement with the experiments, a maximum resistance reduction of 1% could be achieved by trimming the original KCS hull $\theta = 0.25^\circ$ to bow for medium and design speed. For the slow steaming speed, the resistance reduction kept nearly constant for all bow-down trim angles. Finally, the RANSE simulation results for the total resistance of the original KCS were in good agreement with the experimental measurements.

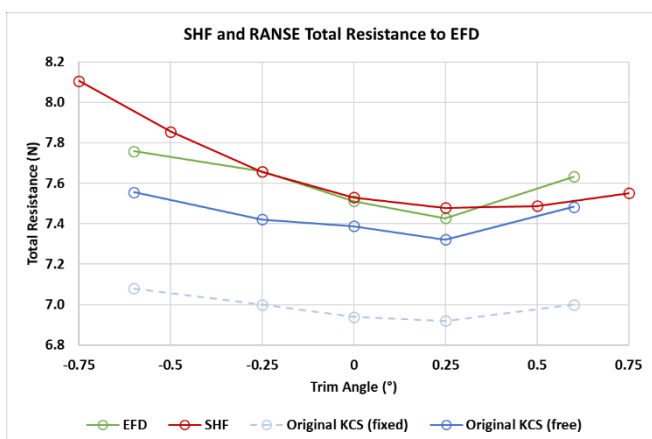


Figure 15. Total resistance comparison for numerical and experimental results

Figure 15 compares the numerical results, i.e. the potential flow calculations and the RANSE calculations with the KCS fixed and free for sinkage and trim, with the experiments. Due to the wave making resistance coefficient correction applied to the potential flow results, the total resistance agrees well with the experiments. The RANSE computations with an active DFBI model predicted the total resistance with an error of under 3% compared to the experiments. The fixed KCS simulation results, however, showed an error of around 8.5%. This suggests, that the effect of the dynamic sinkage and trim plays an important role, which should be included in such trim studies. Further, it can be noted that the RANSE trend prediction is more accurate compared to the potential flow results.

3.2 KCS bulbous bow designs

For the KCS bulbous bow variation, the results evaluation was again based on the wave resistance and the total resistance. Performing calculations for a high number of different KCS designs allowed deriving an improved bulbous bow design, which led to the minimization of energy losses associated with the generation of waves.

Figure 16 shows the impact of an adapted bulbous bow on the wave making resistance by plotting the resistance reduction for each speed at each trim angle as percentage improvement (right axis). The results show that the bulbous bow variation has a larger impact for the KCS operating in bow-up trim conditions. The largest improvement of around 2.7% was achieved for a bow-up trim angle of $\theta = -0.5^\circ$ for the slow steaming speed. This indicates that even though the immersed transom of the KCS dominates the generation of waves, a re-design of the bulbous bow can still have a significant impact on the wave making resistance.

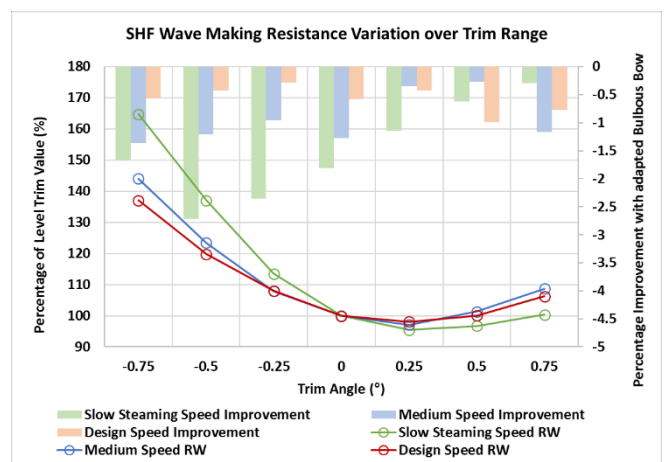


Figure 16. Wave making resistance comparison including possible improvement by adapted bulbous bow

As outlined above, the fraction of the wave making resistance on the total resistance was around 5% for

the slow steaming speed, thus the impact of the bulbous variation on the total resistance was small. The possible improvements for the total resistance are shown in Figure 17.

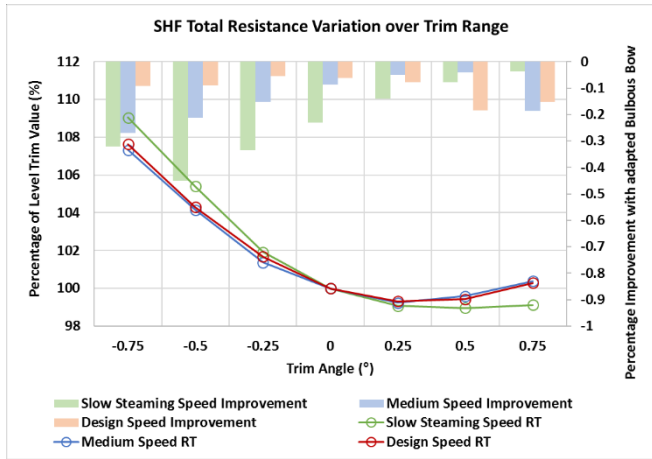


Figure 17. Total resistance comparison including possible improvement by adapted bulbous bow

Similar to the improvements in the wave making resistance, the largest reduction of total resistance could be achieved for bow-up trim angles. For the optimum trim angle of $\theta = 0.25^\circ$ only a minor reduction of around $\Delta R_{TM} = 0.14\%$ was found at slow steaming speed.

Due to the low variation of the results, it was not expected that the weight-based results pool analysis would show larger improvements for different operational profiles. Table 4 presents the combined improvements in total resistance of the trim optimization and the bulbous retrofit for four operational profiles of varying speeds.

Table 4 Best design candidates for different operational profiles

Profile #	Speed Weights			KCS Design	@ θ (°)	$\Delta R_{TM}^{Profile}$ (%)
	t_{v1}	t_{v2}	t_{v3}			
1	2/3	1/6	1/6	D33	0.25	1.14
2	1/6	2/3	1/6	D10	0.25	0.82
3	1/6	1/6	2/3	D24	0.25	0.73
4	1/3	1/3	1/3	D24	0.25	0.75

The table lists the speed weights, the KCS design number (out of 40) for which the improved resistance was calculated, the ideal trim angle and the combined total resistance improvement. Profile #1 represents the KCS operating in slow steaming conditions 66% of its time at a speed of 18 knots. This profile type returns the largest improvements of $\Delta R_{TM} = 1.14\%$ compared to level trim operation for Design 33. For the other profiles, the total savings were below 1%.

Figure 18 highlights the importance of including a dynamic motion model in the RANSE simulations. Whereas the total resistance prediction for the fixed ship simulations did not agree with the experiments

and the potential code computations, the results accuracy increased when including 2-DOF motions. The minor performance increase (here shown at design speed) predicted by the potential solver is not reflected for all trim angles in the RANSE simulations. This could be due to the initial error of the RANSE simulations of around 3%.

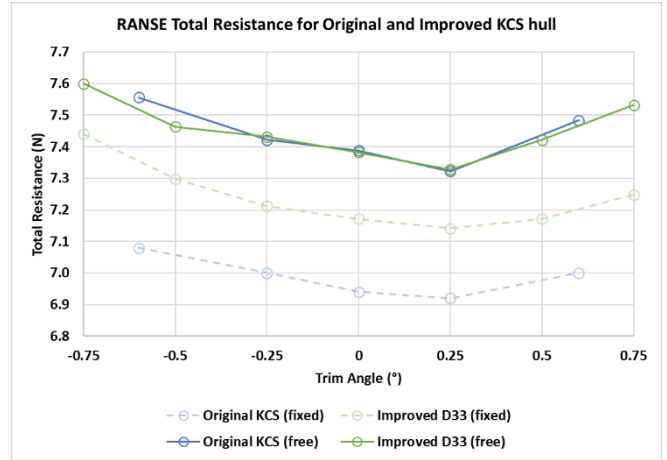


Figure 18. Total resistance comparison including possible improvement by adapted bulbous bow

In order to analyze the best bulbous bow designs (see Table 4) from a geometric point of view, Table 5 presents the change of the bulbs in length, width and tip height compared to the original KCS design.

Table 5 KCS bulbous bow design specifications

Design #	Bulb Length dx (m)	Bulb Width dy (m)	Bulb Tip Height dz (m)
Original	0	0	0
D33	0.891	-0.484	-0.422
D10	-0.188	0.063	-1.313
D24	0.469	0.156	-1.406

All bulbous designs show a reduction in bulb tip height when operated at a trim angle of $\theta = 0.25^\circ$. KCS Design 33 has an increased bulb length of $dx = 0.891 m$.

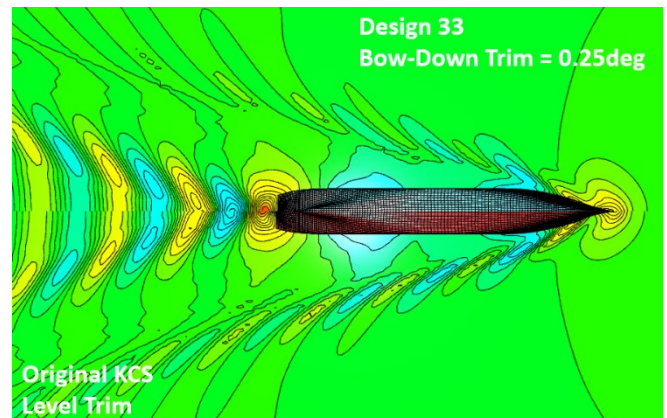


Figure 19. Comparison of KCS design 33 and KCS original design

As can be seen in Figure 19, the presence of the extended bulb generates a slightly longer and shallower bow wave which then results in an improved fore shoulder wave pattern. Further, the emerging transom, due to the forward trim, produced a slightly shallower wake field.

4 CONCLUSION

This paper presented a trim methodology study by combining experimental towing tank testing, potential flow and RANSE flow simulations. The nominal performance of the Kiso Container Ship (KCS) was investigated including a numerical bulbous bow shape variation and its influence in combination with the trim study to find an optimal fore ship design for adverse operating conditions. Thus, it was shown that the combined effort of improving the vessel's floating position (trim) with the simultaneous retrofit of local geometry features, such as the bulbous bow, improved the ship's performance.

In total, 868 numerical simulations were performed for 40 KCS designs with a varying bulbous bow design. The potential flow solver was used to compute the wave making resistance of the KCS for different speeds and trim angles and has proven to make accurate predictions on a fine panel mesh. Due to its short run time the solver was used for a large number of simulations in order to create a sufficient results pool. The solver was able to reproduce the effect of different trim angles on the wave making resistance and was successfully validated by experimental results.

The RANSE simulations were run to predict the total resistance of the KCS without making use of empirical formulations, i.e. the ITTC-1957 frictional correlation line. Results have shown that the RANSE simulations follow the total resistance trend, predicted by the experimental tests, more accurately. However, the RANSE results also show a larger error compared to the corrected potential flow results, thus it remains difficult to judge the predictions made for the bulbous bow variation study. Further, the RANSE simulations showed that the results accuracy was highly dependent on the quasi steady-state ship motions, i.e. dynamic sinkage and trim.

The assessment of the results pool was performed by introducing a weighting method that allowed extracting an improved KCS design for certain operational conditions. Results showed that a bow-down trim of $\theta = 0.25^\circ$ was the most beneficial condition for all three investigated speeds. The total resistance of the original KCS could be reduced by $\Delta R_{TM} = 1.0\%$, which was also validated by the experimental test series. The bulbous variation study yielded only small improvements in operational performance of up to $\Delta R_{TM}^{Profile} = 1.14\%$, for a slow steaming operational profile for the adapted KCS design 33.

5 ACKNOWLEDGEMENT

The authors would like to thank Flowtech International AB for the free access to Shipflow for this study. The numerical RANSE results were obtained using the EPSRC funded ARCHIE-WeSt High Performance Computer (www.archie-west.ac.uk). EPSRC grant no. EP/K000586/1.

6 REFERENCES

Filip, G. et al., 2013. Bulbous Bow Retrofit of a Container Ship Using an Open-Source Computational Fluid Dynamics (CFD) Toolbox. Transactions - Society of Naval Architects and Marine Engineers 122, 1(V), pp. 244–262.

Flowtech User Support, 13 December 2017. Re: KCS bulbous bow study. Type to support@flowtech.se.

Flowtech International Ab, 2017. "Shipflow 6.3 User's Manual".

ITTC Practical Guidelines for Ship CFD Application, 2011, 7.5 – 03 – 02 – 03, p. 11.

Reichel, M., Minchev, a. & Larsen, N.L., 2014. Trim Optimization - Theory and Practice. TransNav, the International Journal on Marine Navigation and Safety of Sea Transportation, 8(3), pp. 387–392. Available at: http://www.transnav.eu/Article_Trim_Optimisation_-_Theory_and_Reichel,31,521.html.

Shivachev, E., Khorasanchi, M. & Day, A.H., 2017. Trim Influence on Kiso Container Ship (KCS); An Experimental and Numerical Study In Proceedings of the ASME 2017 36th International Conference on Ocean, Offshore and Arctic Engineering. Trondheim, pp. 1–7.

SIEMENS, 2017. "User guide STAR-CCM+ Version 12.02.009,"

Vroegrijk, E., Whitworth, S. & Caldas, A., 2015. Validation of Bulbous Bow Optimisation by Viscous CFD.

Wagner, J., Binkowski, E. & Bronsart, R., 2014. Scenario based optimization of a container vessel with respect to its projected operating conditions. International Journal of Naval Architecture and Ocean Engineering, 6 (2), pp. 496–506. Available at: <http://dx.doi.org/10.2478/IJNAOE-2013-0195>.